

Active, passive, and motor imagery paradigms: component analysis to assess neurovascular coupling

Angela S. M. Salinet,¹ Thompson G. Robinson,^{1,2} and Ronney B. Panerai^{1,2}

¹Department of Cardiovascular Sciences, University of Leicester, Leicester, United Kingdom; and ²Biomedical Research Unit in Cardiovascular Sciences, National Institutes for Health Research, Leicester, United Kingdom

Submitted 7 December 2012; accepted in final form 21 February 2013

Salinet AS, Robinson TG, Panerai RB. Active, passive, and motor imagery paradigms: component analysis to assess neurovascular coupling. *J Appl Physiol* 114: 1406–1412, 2013. First published February 28, 2013; doi:10.1152/jappphysiol.01448.2012.—The association between neural activity and cerebral blood flow (CBF) has been used to assess neurovascular coupling (NVC) in health and diseases states, but little attention has been given to the contribution of simultaneous changes in peripheral covariates. We used an innovative approach to assess the contributions of arterial blood pressure (BP), PaCO₂, and the stimulus itself to changes in CBF velocities (CBFv) during active (MA), passive (MP), and motor imagery (MI) paradigms. Continuous recordings of CBFv, beat-to-beat BP, heart rate, and breath-by-breath end-tidal CO₂ (EtCO₂) were performed in 17 right-handed subjects before, during, and after motor-cognitive paradigms performed with the right arm. A multivariate autoregressive-moving average model was used to calculate the separate contributions of BP, EtCO₂, and the neural activation stimulus (represented by a metronome on-off signal) to the CBFv response during paradigms. Differences were found in the bilateral CBFv responses to MI compared with MA and MP, due to the contributions of stimulation ($P < 0.05$). BP was the dominant contributor to the initial peaked CBFv response in all paradigms with no significant differences between paradigms, while the contribution of the stimulus explained the plateau phase and extended duration of the CBFv responses. Separating the neural activation contribution from the influences of other covariates, it was possible to detect differences between three paradigms often used to assess disease-related NVC. Apparently similar CBFv responses to different motor-cognitive paradigms can be misleading due to the contributions from peripheral covariates and could lead to inaccurate assessment of NVC, particularly during MI.

cerebral hemodynamics; neurovascular coupling; transcranial Doppler ultrasound

NEUROVASCULAR COUPLING (NVC) is the cerebral mechanism responsible for linking neuronal activity, cerebral metabolism, and regional cerebral blood flow (CBF) (9, 26). Mediated by a variety of biochemical factors (such as K⁺, NO, and adenosine), neuronal activity leads to dilatation of cerebral arterioles and capillaries followed by an increase in CBF (19, 25). Therefore it is often assumed that CBF changes associated with the metabolic demand generated by a localized increase in cerebral activity are an accurate measurement of underlying neuronal activity (18). Several paradigms have been developed to assess cerebral hemodynamic responses as a predictor of neuronal activity (1, 6, 10, 12, 13, 15, 20, 39). In particular, sensorimotor paradigms have become increasingly popular in the field of neuronal recovery studies, since impairment, preservation, and rehabilitation of sensorimotor function is a piv-

otal issue in many neurological disorders. Over the years, transcranial Doppler ultrasonography (TCD) has been widely used to detect CBFv modulation during neural activation, as it provides continuous information of the dynamic CBFv adjustments and its facility in incorporating peripheral hemodynamics monitoring.

Neural activation studies have provided useful information regarding the adaptive mechanisms of cerebral hemodynamics after stroke (7, 21, 35, 36), as well as in Parkinson's (28) and Alzheimer (16) diseases. One important limitation of previous studies though is that covariates of the CBF response, such as influences of changes in blood pressure (BP) and PaCO₂, have not been taken into account. It is possible that the interplay of other cerebral mechanisms (cerebral autoregulation and cerebrovascular reactivity) and the contribution of covariates (BP and PaCO₂) may affect the accuracy of the raw CBF response in representing underlying cerebral activity (4). To derive more robust NVC measures, Panerai et al. (24) have recently proposed an innovative methodological approach to assess the individual contribution of BP, EtCO₂, and the metabolic stimulus to the CBF responses. This new approach has considerable potential to improve the sensitivity and overall diagnostic accuracy of NVC studies in stroke. As a first step, we analyzed the dynamic CBFv response to active (MA), passive (MP), and motor imaginary (MI) paradigms in a healthy older population to test the hypotheses that 1) these different paradigms stimulate the brain in a similar fashion and 2) the contribution of BP and PaCO₂ is the same for different paradigms.

METHODS

Research participants. A total of 19 participants (age ≥ 45 yr), without vascular risk factors and without symptoms or history of cardiovascular or cerebrovascular disease, were recruited from University staff and their relatives. An additional exclusion criterion comprised physical disease in the upper limb. All subjects were right-handed according to the Edinburgh Handedness Inventory (23). The study was approved by the Nottingham Research Ethics Committee 1, United Kingdom (Ref:11/EM/0016), and each volunteer gave written informed consent.

Brain activation paradigms. The MA paradigm consisted of repetitive flexion and extension of the elbow, given by the sound of a metronome at frequency of 1 Hz. Subjects were instructed to move within a range of movement of $\sim 90^\circ$, to ensure that there was no associated major shoulder movement. The MP paradigm consisted of an examiner moving the subject's elbow within a similar range and rate to the active paradigm; subjects were instructed to relax and not resist or attempt to move the arm. During the rest and recovery periods, the examiner kept hold of the participant's arm. The MI paradigm was also a metronome-paced activity in which the participants imagined that they were actively moving their elbow with the eyes closed. An electrical signal indicating when the metronome was on or off was also recorded.

Address for reprint requests and other correspondence: A. Salinet, Trent Stroke Research Network Office, Level 0 Victoria Bldg., Leicester Royal Infirmary, LE1 5WW, UK. (e-mail: asms2@le.ac.uk)

Procedure. The study was carried out in a quiet and temperature-controlled (22–24°C) research laboratory while the participants were in a supine position. All volunteers had abstained from caffeine, alcohol, and nicotine for 12 h before the measurement. Bilateral insonation of the middle cerebral arteries (MCAs) was performed using ultrasound Doppler (Viasys Companion III; Viasys Healthcare) with a 2-MHz probe, which was secured in place using a head frame. Beat-to-beat BP was recorded continuously with a Finapres device (Ohmeda 2300; Finapres, Louisville, CO) attached to the middle finger of the left hand. Heart rate (HR) was recorded using a 3-lead electrocardiogram (ECG), and end-tidal CO₂ (EtCO₂) was measured via nasal prongs (Salter Labs) by a capnograph (Capnograph Plus).

The recording procedure was described previously (30). Briefly, after a period of 15 min stabilization, the paradigms were performed twice in random order. One measurement set had a total duration of 4 min: recording started with a 90-s baseline phase, and then the paradigm was performed over 60 s, with a 90-s recovery phase. Detailed instructions were given before measurements. Movement was performed only with the right arm. Data were simultaneously recorded onto a data acquisition system (PHYSIDAS, Medical Physics Group) at a sampling rate of 500 samples/s. The stimulus signal (SS) using the electrical output from the metronome was added to the ensemble.

Data analysis. CBFv, BP, HR, and EtCO₂ signals were visually inspected to identify artefacts and noise, and narrow spikes (<100 ms) were removed by linear interpolation. The CBFv channels were subjected to a median filter and all signals were filtered by a low pass filter (zero-phase eighth-order Butterworth filter) with a cutoff frequency of 20 Hz. R-R interval was then automatically marked from the ECG, and mean BP and CBFv values were calculated for each beat. Linear interpolation was used to obtain estimates of EtCO₂ synchronized to the end of each cardiac cycle. Beat-to-beat data were spline interpolated and resampled at 5 Hz to produce signals with a uniform time base.

A multivariate autoregressive-moving average (ARMA) model was used to represent the influence of the inputs (BP, EtCO₂, and SS) on output (CBFv). As described in APPENDIX and in previous work (24), the ARMA model allows quantification of the simultaneous influences of BP, EtCO₂, and SS to the CBFv response to stimulation. Briefly, the separate contributions of BP, EtCO₂, and stimulus to CBFv response were obtained as model predictions, with the use of ARMA coefficients. The order of these models, representing the number of past samples adopted for the autoregressive (AR) and moving average (MA) terms, was thoroughly considered as described in APPENDIX. The beginning of stimulation was used as the point of synchronism to obtain population mean and SD curves for each separate contribution (BP, EtCO₂, stimulus) for the ipsilateral and contralateral hemispheres.

Statistical analysis. CBFv response patterns from two executions of each paradigm for each subject were qualitatively compared and the maneuver that achieved the highest amplitude of contralateral CBFv response was chosen to represent the participant's response (31). Mean CBFv values were extracted from the 30 s preceding the paradigm for baseline. CBFv responses to stimulation were calculated at the first 10 s (for evaluating the initial impact of the paradigms) and last 30 s of each paradigm expressed as time points *t*₁₀ and *t*₃₀, respectively. For the same time intervals, the mean of the predicted contributions of BP, EtCO₂, and SS to CBFv responses were also calculated. All parameters were expressed as percentages (%) of baseline values.

Using two-way repeated measures ANOVA, baseline values of CBFv were compared between MA, MP, and MI paradigms and between the side of recording (ipsi- and contralateral hemispheres). At the selected time points (*t*₁₀ and *t*₃₀), two-way repeated measures ANOVA with paradigms (MA, MP, MI) and side of recording (right, left hemispheres) as the within-factor for CBFv variations and for the predicted contributions of BP, EtCO₂, and SS to CBFv responses was

used. Tukey's honest significant difference test was adopted for post hoc analyses. A value of $P < 0.05$ was adopted to indicate statistical significance. A correlation analysis was performed to compare the similarity of the values of variables at the *t*₁₀ and *t*₃₀ time points.

RESULTS

Two participants were removed from the study due to poor insonation of the temporal acoustic window. No data were discarded following visual inspection. Therefore data from 17 subjects (12 male) were included in this study. Included subjects had a mean (SD) age of 64.9 (4.9) yr and Edinburgh Inventory of 91.0 (2.1)%. Baseline peripheral and cerebral hemodynamic parameters were systolic BP 124 (2.9) mmHg, diastolic BP 82 (1.0) mmHg, HR 65 (0.7) beats/min, right MCA CBFv 59.0 (1.9) cm/s, and left MCA CBFv 61.9 (2.1) cm/s. Baseline EtCO₂ was 39 (1.7) mmHg.

Ninety-seven of the 102 recordings analyzed showed satisfactory model fitting as given by the comparison between model-predicted CBFv responses and the real data (24). Five recordings from two subjects resulted in poor fitting using the original model orders (orders [2,4,1,1]). However, adjusting model orders, mainly by increasing the order of the stimulus terms, solved this problem (APPENDIX).

Temporal pattern of CBFv responses and its contributors. Two-way ANOVA did not show significant CBFv differences between the three paradigms or between ipsi- and contralateral hemispheres at baseline. During paradigms, CBFv showed bilaterally a steep peaked rise, followed by a plateau phase, which outlasted the duration of stimulation (Fig. 1, *A* and *B*). On the other hand, the contribution of SS (Fig. 1, *C* and *D*) yielded a much simpler pattern, with a steady plateau and similar duration as the CBFv response. The contributions of EtCO₂ (Fig. 2, *A* and *B*) and BP (Fig. 2, *C* and *D*) showed both positive and negative values. EtCO₂ increased before MI paradigm onset and contributed to the CBFv rise, especially in the contralateral response (Fig. 2*B*). EtCO₂ levels decreased gradually during MI and MA paradigms (reaching a minimum after the end of paradigms performances; Fig. 2, *A* and *B*). In all three paradigms, BP showed a clear peak at the beginning of stimulation coinciding with the initial peak in the CBFv response (Fig. 2, *C* and *D*).

CBFv responses. The amplitude of CBFv and the input parameters variation at *t*₁₀ and *t*₃₀ are summarized in Table 1. At *t*₁₀, no significant difference was found. At *t*₃₀, two-way ANOVA showed significant differences ($F = 76.2$, $P = 0.04$) in CBFv response between the three paradigms. Post hoc comparisons revealed significant differences (Tukey's post hoc $P = 0.04$) between MI and MP CBFv responses in the contralateral hemisphere and showed a trend toward a significant difference during MI compared with the MA paradigm (Tukey's post hoc $P = 0.05$). A similar trend for a reduced CBFv response during MI was also present in the ipsilateral responses (Table 1) showing a marginal significance compared with the MP paradigm ($P = 0.05$). The correlation between *t*₁₀ and *t*₃₀ CBFv values ranged from 0.24 (motor imagery, $P = 0.5$) to 0.52 (active, $P = 0.2$) for ipsilateral responses and from -0.03 (motor imagery, $P = 0.9$) to 0.57 (active, $P = 0.1$) for contralateral responses, therefore not showing any strong relationships.

Contribution of individual inputs to CBFv responses. Table 2 gives the distributions of explained variance for each input.

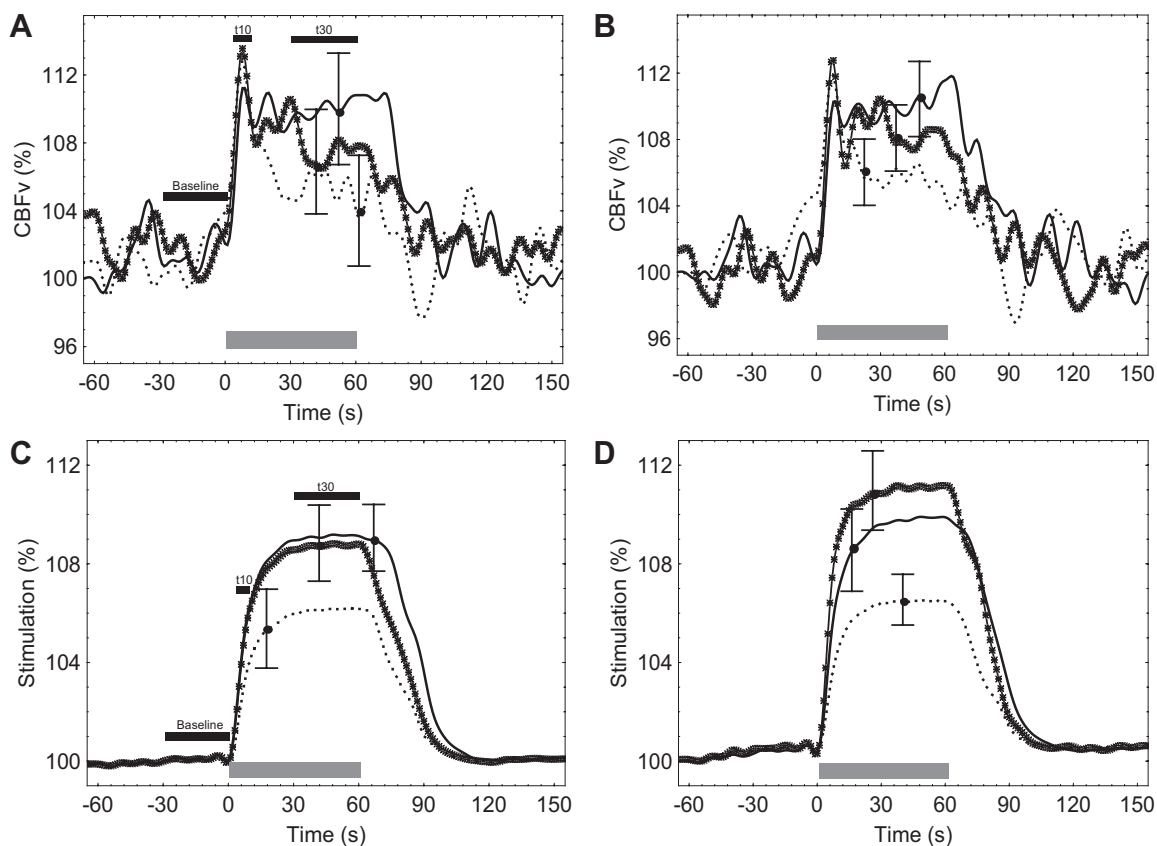


Fig. 1. Population averages of changes in ipsilateral (A) and contralateral (B) cerebral blood flow velocity (CBFv) responses and stimulus contribution (C: ipsilateral; D: contralateral) to active (continuous line + symbol), passive (continuous line), and motor imagery (dotted line). The gray horizontal bar shows the duration of stimulation. Error bar represents the largest ± 1 SE at the point of occurrence.

Although Table 2 is presenting higher values for the stimulus contribution in all paradigms, Tukey's post hoc showed significant differences only between active (MA) contralateral BP and stimulus contribution ($F = 4$, $P = 0.03$). A significant difference was also found between passive contralateral BP and EtCO₂ contributions ($F = 4$, $P = 0.03$, Tukey's post hoc $P = 0.04$). Note that in each paradigm, the total variance explained by the model is given for ipsilateral and contralateral hemispheres. Nevertheless, a better insight about the contribution of each input is gained by studying their temporal patterns (Fig. 1, C and D, and Fig. 2) and the corresponding values of t_{10} and t_{30} (Table 1).

No significant difference between the three paradigms was found in the BP and EtCO₂ contribution at t_{10} and t_{30} (Table 1). However, two-way ANOVA revealed differences of stimulus contribution on CBFv responses at both t_{10} and t_{30} ($F = 14.8$, $P = 0.03$ and $F = 42.03$, $P = 0.04$, respectively). At t_{10} , stimulus contributions differed significantly between MI and MA (Tukey's post hoc $P = 0.04$) and MP paradigms (Tukey's post hoc $P = 0.03$) in the ipsilateral hemisphere (Table 1). Moreover, contralateral stimulus increase during MI was significantly lower compared with MA (Tukey's post hoc $P = 0.001$) and MP (Tukey's post hoc $P = 0.007$) paradigms (Table 1). At t_{30} , contralateral change in MI stimulus was also reduced compared with the other two paradigms using Tukey's post hoc (MA $P = 0.02$, MP $P = 0.03$) (Table 1). The contribution of BP showed no or poor association between t_{10} and t_{30} . Ipsilateral correlation ranged from 0.28 (motor imag-

ery, $P = 0.4$) to 0.51 (passive, $P = 0.1$), whereas contralateral ranged between -0.01 (motor imagery, $P = 0.9$) and 0.42 (passive, $P = 0.2$). On the other hand, with the exception of the EtCO₂ contribution during ipsilateral motor imagery ($r = 0.3$, $P = 0.3$), highly significant correlations were found in EtCO₂ and stimulus ranging from 0.76 (contralateral motor imagery EtCO₂ contribution) to 0.93 (ipsilateral passive SS contribution).

DISCUSSION

To our knowledge, this is the first time that the individual influences of the active, passive, and motor imagery stimulus and other peripheral covariates on CBFv responses have been assessed and compared by multivariate modeling (see APPENDIX). Although the temporal course of beat-to-beat CBFv response across the three paradigms is consistent with previous studies (24, 30, 31), CBFv response and the individual CBFv inputs were significantly different during motor imagery compared with active and passive motor responses. Stimulus was shown to be the major contributor of CBFv increases during the paradigm performance ranging from 103.0 (2.4)% to 110.6 (5.2)%, as detailed in Tables 1 and 2. These findings suggest that as well as differences in the metabolic components of the CBFv response caused by MA, MP, and MI paradigms, rapid influences of peripheral hemodynamics (blood pressure and PaCO₂) may also be involved in cerebral hemodynamic changes. The fluctuating BP and EtCO₂ modulation suggests that both

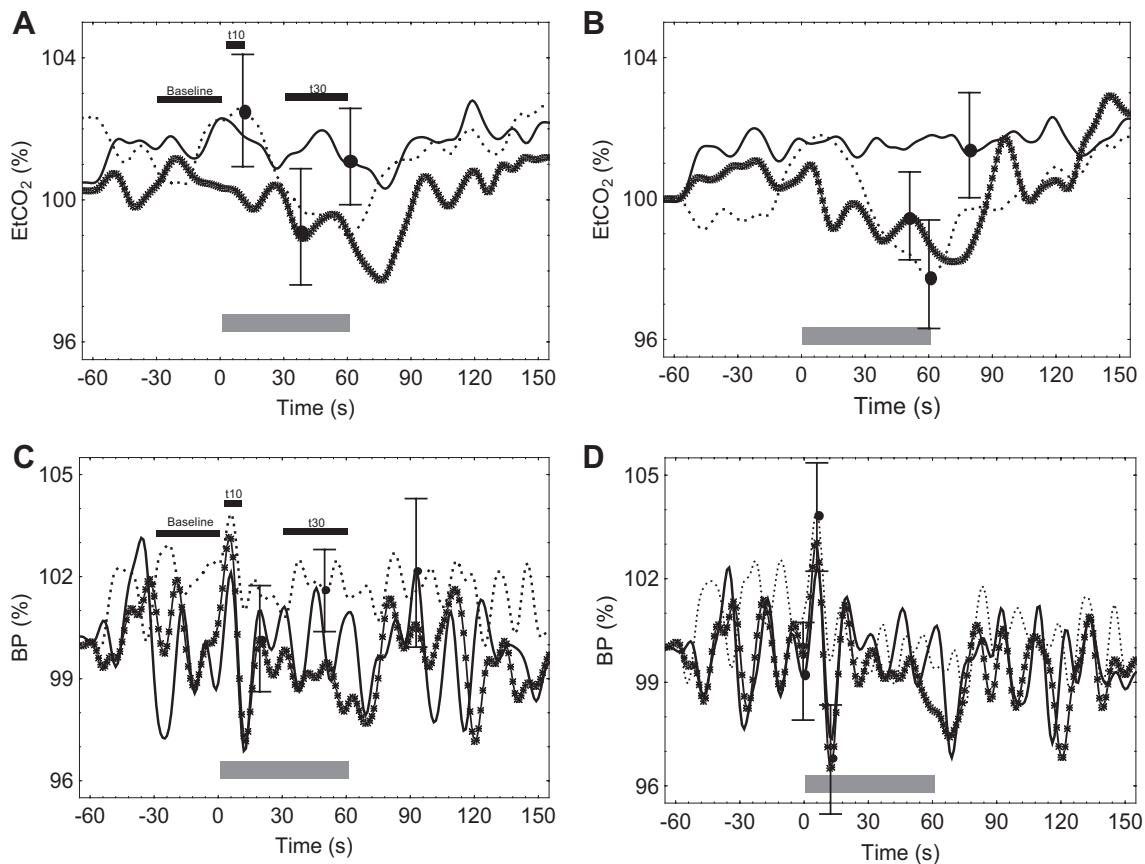


Fig. 2. Population averages of the contributions of end-tidal CO₂ (EtCO₂) (A: ipsilateral; B: contralateral) and blood pressure (BP) (C: ipsilateral; D: contralateral) to CBFv response to active (continuous line + symbol), passive (continuous line), and motor imagery (dotted line). The gray horizontal bar shows the duration of stimulation. Error bar represents the largest ± 1 SE at the point of occurrence.

parameters contributed to either increasing or decreasing the CBFv response during paradigms.

The initial temporal pattern of CBFv response, involving a steep bilateral increase, is consistent with former TCD studies using a broad variety of brain activation paradigms (4, 14, 15, 22, 24, 29, 30, 32, 37). In keeping with our results, Duscheck et al. (15) found the effects of BP on CBFv responses during arithmetic processing were also more pronounced during the first second of the response. From our analysis, it could be seen

that this fast CBFv increase was mainly a response of a sharp BP rise rather than a neural metabolic response during the three paradigms, indicating that the first 10 s of CBFv response should not be used as a solo index of NVC, a concern also raised by Panerai et al. (24). In addition to the observed BP contribution, greater influences of PaCO₂ were also observed during MI and MA CBFv (Fig. 2, A and B), contributing to decreasing CBFv during such paradigms. Most studies have ignored the influences of breath-by-breath PaCO₂, although

Table 1. Comparison of CBFv and separate contributions from BP, EtCO₂, and the stimulus during active, passive and motor imagery paradigms at the beginning (t10) and end (t30) of stimulation

CBFv and Contributors	Ipsilateral			Contralateral		
	Active	Passive	MI	Active	Passive	MI
<i>t10</i>						
CBFv, %	108.3 (4.9)	108.0 (5.0)	109.9 (5.6)	108.9 (4.8)	107.7 (4.2)	107.6 (5.3)
BP, %	100.2 (1.7)	99.7 (3.5)	100.8 (2.5)	100.2 (1.9)	100.3 (2.4)	100.9 (3.3)
EtCO ₂ , %	100.5 (1.4)	101.8 (1.6)	102.0 (1.7)	100.7 (1.4)	101.0 (2.0)	101.9 (4.0)
Stimulus, %	104.1 (2.9)	105.0 (2.4)	103.0 (2.4)*	106.8 (4.3)	105.1 (2.1)	103.2 (1.8)*
<i>t30</i>						
CBFv, %	107.3 (8.0)	109.2 (8.1)	104.3 (7.0)#	108.3 (6.9) ∞	110.1 (6.7)	105.9 (4.7)+
BP, %	100.0 (2.9)	100.1 (2.6)	101.0 (1.8)	99.2 (2.2)	100.1 (2.0)	99.9 (1.5)
EtCO ₂ , %	99.7 (5.0)	101.3 (9.3)	99.9 (5.2)	98.5 (7.1)	100.4 (4.7)	99.1 (5.0)
Stimulus, %	108.7 (5.9)	109.0 (4.6)	106.1 (5.4)	110.6 (5.2)	109.4 (3.6)	106.0 (4.0)*

Values are means (SE). CBFv, cerebral blood flow velocity; BP, mean arterial blood pressure; EtCO₂, end tidal CO₂; MI, motor imagery. * $P < 0.05$, Tukey's post hoc for differences between MI and active, and MI and passive paradigms; # $P = 0.05$, Tukey's post hoc for differences between passive and MI. + $P < 0.05$, Tukey's post hoc for differences between passive and MI. $\infty P = 0.05$, Tukey's post hoc for differences between active and MI.

Table 2. Percent of total CBFv variance explained by model (V_{MOD}) and corresponding distribution of individual contribution of input variables as percent of V_{MOD} (see APPENDIX)

	Variance Contribution, %					
	Ipsilateral			Contralateral		
	Active	Passive	MI	Active	Passive	MI
V_{MOD}	62.8 (21.3)	61.7 (19.4)	55.9 (20.8)	71.6 (15.8)	74.5 (14.8)	64.5 (16.3)
BP	25.5 (19.2)	25.8 (23.6)	30.8 (24.7)	23.2 (18.6)+	25.7 (22.6)*	35.3 (28.6)
EtCO ₂	30.9 (25.3)	28.7 (26.7)	29.4 (29.6)	29.4 (24.1)	25.5 (19.5)	21.4 (22.8)
Stimulus	43.6 (21.4)	45.5 (26.6)	39.8 (20.6)	47.4 (21.7)	48.8 (25.4)	43.3 (25.3)

Values are means (SD). + $P < 0.05$, Tukey's post hoc for differences between BP and stimulus contribution. * $P < 0.05$, Tukey's post hoc for differences between BP and EtCO₂ contribution.

Moody et al. (22) and Ances et al. (3) showed that PaCO₂ variations during brain activation may modulate cerebrovascular responses. The significant variation of systemic hemodynamics might reflect the fact that both paradigms impose greater demands on attention thus leading participants to higher levels of stress and associated changes to their breathing pattern.

Functional imaging studies have suggested the use of MI and MP paradigms to induce neural activation in areas normally involved in the control of voluntary motor activity (5, 27, 38). In a previous study we have demonstrated that CBFv responses to active, passive, and motor imagery have similar and reproducible patterns of CBFv response in healthy volunteers (30, 31), with no significant differences between paradigms. However, when the contribution of each stimulus was extracted from the raw CBFv responses, differences between paradigms could be detected showing a greater sensitivity of model derived estimates to detect differences between paradigms (Fig. 1, C and D). On the other hand, the lack of significant differences at $t30$ is possible due to limitation in statistical power since a similar trend was observed in that case (Table 1). While all paradigms led to CBFv increases, the MI stimulus showed a lesser contribution to the CBF response than the motor paradigms, which is in agreement with previous reports (27, 38). Although active and MI share common functional circuits, MI leads to smaller BOLD signals (38) and motor-evoked potentials (27) as cortical excitability increases with increases in task complexity.

In this study, and in agreement with the literature (5, 11, 20, 40), MA and MP paradigms led to similar CBFv responses. The similarity persisted even when the contribution of other variables was excluded from the raw CBFv response. While both active and passive paradigms during CBF (or CBFv) measurement may be used to obtain information about the mechanisms of neuronal adaptation after disease states (8, 21, 33, 34), our experience would recommend the use of passive paradigms to study the recovery of neuronal function as it allows the inclusion of patients with various degrees of motor impairment in all disease stages. Moreover, we have previously demonstrated that the passive paradigm leads to more reliable cerebral hemodynamic responses compared with voluntary movement (31).

A number of limitations of the present study should be noted. First, in the absence of EMG recordings, voluntary muscular activity during the passive motor paradigm could not be ruled out. However, this paradigm has shown fair to moderate reproducibility for CBFv responses in a previous

study (31). Second, TCD cannot be used to discriminate focal CBF during neural activation. It is possible that the paradigms we adopted did not provide just a focal sensorimotor stimulation but also a nonspecific mental stimulus involving attention, concentration, and motivation. However, since TCD has a good temporal resolution in spite of a relatively poor spatial resolution, it may serve as a complementary tool for investigating cortical motor control in normal and disease-related states. Indeed, the similarities shown in this study are in keeping with previous functional imaging data (5, 17, 40). Although the choice of parameters $t10$ and $t30$ was somewhat arbitrary, CBFv correlation analysis suggested that they have the potential to provide independent information. As hypothesized above, $t10$ CBFv responses seem to be mostly driven by BP variations, whereas $t30$ may reflect more metabolic response of the paradigms. A sensitivity analysis (not reported) also indicated that $t10$ did not change significantly compared with other alternatives in the range 0–15 s (0–5, 5–10, 0–15). Another limitation results from TCD measuring CBFv rather than absolute CBF. Measurements of CBFv will be proportional to changes in blood flow only if the diameter of the insonated vessel remains constant (2). Finally, internal carotid stenosis was not examined in all participants. Future neurophysiological research in this area could certainly benefit from an extracranial vascular evaluation.

In conclusion, our first hypothesis was rejected, since motor cognitive paradigms did not stimulate NVC in a similar fashion. On the other hand, our second hypothesis could not be rejected since the contribution of peripheral covariates did not differ between paradigms. These findings have important implications for the interpretation of previous neurovascular coupling studies and for the design of future studies assessing impairment of neurovascular coupling due to disease and its natural history. In particular, the use of MI paradigms to assess patients' CBF and monitor their recovery is discouraged due to its poorer response to stimulation compared with MA and MP paradigms. Instead, the passive paradigm is recommended for this purpose given its similar responses to active paradigms, its superior reproducibility of CBFv responses (30), and lesser dependence on patient cooperation. The new approach proposed to separate the contributions of BP, PaCO₂, and stimulation from the raw CBF response shows considerable potential to increase the diagnostic accuracy of NVC assessment and hence warrants further investigation.

APPENDIX

Estimation of parameters in multivariate ARMA modeling. A multivariate autoregressive-moving average (ARMA) model was adopted to express the dependence of CBFV, $v(t)$ as a function of ABP, EtCO₂, and the sensorimotor stimulation, represented by $p(t)$, $c(t)$, and $s(t)$, respectively:

$$v(n) = \sum_1^{N_v} a_i v(n-i) + \sum_0^{N_p} b_j p(n-j) + \sum_0^{N_c} d_k c(n-k) + \sum_0^{N_s} g_q s(n-q) \quad (1)$$

where n is the discrete sample number and $[N_v, N_p, N_c, N_s]$ are the model orders for each of the autoregressive (AR) and moving-average (MA) terms in Eq. 1. Here a_i are the AR coefficients and b_j , d_k , and g_q are the MA coefficients. To represent the stimulus signal $s(t)$, the electrical output of a metronome was continuously recorded generating a zero voltage signal when the metronome was OFF and a constant amplitude signal with arbitrary amplitude when the metronome and the maneuver were ON. The model parameters g_q will then reflect the amplitude of the contribution of $s(t)$ to explain changes in $v(t)$.

Identification of suitable model orders $[N_v, N_p, N_c, N_s]$ is a critical step in the use of ARMA models. From previous work (24), initial model orders were [2,4,1,1]. Model coefficients were calculated by least squares and Eq. 1 was used to calculate the model predicted time series of $v(t)$ and the prediction error σ_e from the sum of squared differences in relation to real data. For each combination of model orders, it is possible to calculate the final prediction error (FPE) as

$$\text{FPE} = \sigma_e \frac{N + N_t}{N - N_t} \quad (2)$$

where N is the number of samples in the record and N_t is the total number of model coefficients. The Student's- t value t_k can also be calculated for each estimated coefficient as

$$t_k = \frac{c_k}{\text{SD}_k} \quad k = 1, 2, \dots, N_t \quad (3)$$

with c_k corresponding to the estimated coefficient value and SD_k its standard deviation.

Optimal model orders were identified by the compromise between minimum values of FPE and maximum number of coefficients with significant values of t_k . A multistep, semiautomatic procedure was implemented to examine all combinations of model orders within a set range and select optimal values from inspections of 2 by 2 matrices of FPE and t_k . Finally, for the selected combination of model orders, the quality of model fitting was always confirmed by visual inspection of the predicted temporal pattern of $v(t)$ (Eq. 1) compared with real data.

The fraction of the total $v(n)$ variance explained by the model, V_{MOD} , was calculated from the squared Pearson correlation coefficient between the measured time series of $v(n)$ and model predicted values from Eq. 1. A similar approach was adopted to calculate the relative contribution of each input variable, $p(n)$, $c(n)$, or $s(t)$, as a percentage of V_{MOD} .

GRANTS

A. S. M. Salinet is funded by the Brazilian Ministry of Education (Grant 0411-10-8).

DISCLOSURES

No conflict of interest, financial or otherwise, are declared by the author(s).

AUTHOR CONTRIBUTIONS

A.M.S., T.G.R., and R.B.P. conception and design of research; A.M.S. performed experiments; R.B.P. wrote software; A.M.S. and R.B.P. analyzed data; A.M.S., T.G.R., and R.B.P. interpreted results of experiments; A.M.S. drafted manuscript; T.G.R. and R.B.P. edited and revised manuscript; A.M.S.,

T.G.R., and R.B.P. approved final version of manuscript; A.M.S. prepared figures.

REFERENCES

1. Aaslid R. Visually evoked dynamic blood-flow response of the human cerebral-circulation. *Stroke* 18: 771–775, 1987.
2. Aaslid R, Markwalder T, Nornes H. Non-invasive transcranial Doppler ultrasound recording of flow velocity in basal cerebral arteries. *J Neurosurg* 57: 769–774, 1982.
3. Ances BM, Greenberg JH, Detre JA. The effects of graded hypercapnia on the activation flow coupling response due to forepaw stimulation in α -chloralose anesthetized rats. *Brain Res* 911: 82–88, 2001.
4. Azevedo E, Rosengarten B, Santos R, Freitas J, Kaps M. Interplay of cerebral autoregulation and neurovascular coupling evaluated by functional TCD in different orthostatic conditions. *J Neurol* 254: 236–241, 2007.
5. Blatow M, Reinhardt J, Riffel K, Nennig E, Wengenroth M, Stippich C. Clinical functional MRI of sensorimotor cortex using passive motor and sensory stimulation at 3 Tesla. *J Magn Reson Imaging* 34: 429–437, 2011.
6. Boecker H, Kleinschmidt A, Requardt M, Hanicke W, Merboldt KD, Frahm J. Functional cooperativity of human cortical motor areas during self-paced simple finger movements: A high-resolution MRI study. *Brain* 117: 1231–1239, 1994.
7. Bragoni M, Caltagirone C, Troisi E, Matteis M, Vernieri F, Silvestrini M. Correlation of cerebral hemodynamic changes during mental activity and recovery after stroke. *Neurology* 55: 35–40, 2000.
8. Caramia MD, Palmieri MG, Giacomini P, Iani C, Dally L, Silvestrini M. Ipsilateral activation of the unaffected motor cortex in patients with hemiparetic stroke. *Clin Neurophysiol* 111: 1990–1996, 2000.
9. Carmignoto G, Gomez-Gonzalo M. The contribution of astrocyte signalling to neurovascular coupling. *Brain Res Rev* 63: 138–148, 2010.
10. Diciotti S, Gavazzi C, Della Nave R, Boni E, Ginestroni A, Paoli L, Cecchi P, De Stefano N, Mascalchi M. Self-paced frequency of a simple motor task and brain activation: An fMRI study in healthy subjects using an on-line monitor device. *Neuroimage* 38: 402–412, 2007.
11. Doering TJ, Resch KL, Steuernagel B, Brix J, Schneider B, Fischer GC. Passive and active exercises increase cerebral blood flow velocity in young, healthy individuals. *Am J Phys Med Rehabil* 77: 490–493, 1998.
12. Donahue MJ, Stevens RD, de Boorder M, Pekar JJ, Hendrikse J, van Zijl PCM. Hemodynamic changes after visual stimulation and breath holding provide evidence for an uncoupling of cerebral blood flow and volume from oxygen metabolism. *J Cereb Blood Flow Metab* 29: 176–185, 2009.
13. Droste DW, Harders AG, Rastogi E. Two transcranial Doppler studies on blood flow velocity in both middle cerebral arteries during rest and the performance of cognitive tasks. *Neuropsychologia* 27: 1221–1230, 1989.
14. Duschek S, Schuepbach D, Schandry R. Time-locked association between rapid cerebral blood flow modulation and attentional performance. *Clin Neurophysiol* 119: 1292–1299, 2008.
15. Duschek S, Werner N, Kapan N, del Paso G. AR patterns of cerebral blood flow and systemic hemodynamics during arithmetic processing. *J Psychophysiol* 22: 81–90, 2008.
16. Girouard H, Iadecola C. Neurovascular coupling in the normal brain and in hypertension, stroke and Alzheimer disease. *J Appl Physiol* 100: 328–335, 2006.
17. Guzzetta A, Staudt M, Petacchi E, Ehlers J, Erb M, Wilke M, Kragehlo-Mann I, Cioni G. Brain representation of active and passive hand movements in children. *Pediatr Res* 61: 485–490, 2007.
18. Hamilton NB, Attwell D, Hall CN. Pericyte-mediated regulation of capillary diameter: a component of neurovascular coupling in health and disease. *Front Neuroenergetics* 2: 5, 2010.
19. Iadecola C. Neurovascular regulation in the normal brain and in Alzheimer's disease. *Nat Rev Neurosci* 5: 347–360, 2004.
20. Matteis M, Caltagirone C, Troisi E, Vernieri F, Monaldo BC, Silvestrini M. Changes in cerebral blood flow induced by passive and active elbow and hand movements. *J Neurol* 248: 104–108, 2001.
21. Matteis M, Vernieri F, Troisi E, Pasqualetti P, Tibuzzi F, Caltagirone C, Silvestrini M. Early cerebral hemodynamic changes during passive movements and motor recovery after stroke. *J Neurol* 250: 810–817, 2003.
22. Moody M, Panerai RB, Eames PJ, Potter JF. Cerebral and systemic hemodynamic changes during cognitive and motor activation paradigms. *Am J Physiol Regul Integr Comp Physiol* 288: R1581–R1588, 2005.

23. **Oldfield R.** The assessment and analysis of handedness: The Edinburgh inventory. *Neuropsychologia* 9: 97–113, 1971.
24. **Panerai RB, Salinet ASM, Robinson TG.** Contribution of arterial blood pressure and PaCO₂ to the cerebrovascular responses to motor stimulation. *Am J Physiol Heart Circ Physiol* 302: H459–H466, 2012.
25. **Paulson OB.** Blood brain barrier, brain metabolism and cerebral blood flow. *Eur Neuropsychopharmacol* 12: 495–501, 2002.
26. **Riera JJ, Sumiyoshi A.** Brain oscillations: ideal scenery to understand the neurovascular coupling. *Curr Opin Neurol* 23: 374–381, 2010.
27. **Roosink M, Zijdwind I.** Corticospinal excitability during observation and imagery of simple and complex hand tasks: implications for motor rehabilitation. *Behav Brain Res* 213: 35–41, 2010.
28. **Rosengarten B, Dannhardt V, Burr O, Pohler M, Rosengarten S, Oechsner M, Reuter I.** Neurovascular coupling in Parkinson's disease patients: Effects of dementia and acetylcholinesterase inhibitor treatment. *J Alzheimers Dis* 22: 415–421, 2010.
29. **Rosengarten B, Osthaus S, Auch D, Kaps M.** Effects of acute hyperhomocysteinemia on the neurovascular coupling mechanism in healthy young adults. *Stroke* 34: 446–451, 2003.
30. **Salinet ASM, Panerai RB, Robinson TG.** Effects of active, passive and motor imagery paradigms on cerebral and peripheral hemodynamics in older volunteers: a functional TCD study. *Ultrasound Med Biol* 38: 997–1003, 2012.
31. **Salinet ASM, Robinson TG, Panerai RB.** Reproducibility of cerebral and peripheral haemodynamic responses to active, passive and motor imagery paradigms in older healthy volunteers: a fTCD study. *J Neurosci Methods* 206: 143–150, 2012.
32. **Sato K, Moriyama M, Sadamoto T.** Influence of central command on cerebral blood flow at the onset of exercise in women. *Exp Physiol* 94: 1139–1146, 2009.
33. **Seitz RJ, Hoflich P, Binkofski F, Tellmann L, Herzog H, Freund HJ.** Role of the premotor cortex in recovery from middle cerebral artery infarction. *Arch Neurol* 55: 1081–1088, 1998.
34. **Silvestrini M, Caltagirone C, Cupini LM, Matteis M, Troisi E, Bernardi G.** Activation of healthy hemisphere in poststroke recovery—a transcranial Doppler study. *Stroke* 24: 1673–1677, 1993.
35. **Silvestrini M, Troisi E, Matteis M, Cupini LM, Caltagirone C.** Involvement of the healthy hemisphere in recovery from aphasia and motor deficit in patients with cortical ischemic infarction—a transcranial Doppler study. *Neurology* 45: 1815–1820, 1995.
36. **Silvestrini M, Troisi E, Matteis M, Razzano C, Caltagirone C.** Correlations of flow velocity changes during mental activity and recovery from aphasia in ischemic stroke. *Neurology* 50: 191–195, 1998.
37. **Sitzer M, Knorr U, Seitz RJ.** Cerebral hemodynamics during sensorimotor activation in humans. *J Appl Physiol* 77: 2804–2811, 1994.
38. **Stippich C, Ochmann H, Sartor K.** Somatotopic mapping of the human primary sensorimotor cortex during motor imagery and motor execution by functional magnetic resonance imaging. *Neurosci Lett* 331: 50–54, 2002.
39. **Stroobant N, Vingerhoets G.** Test-retest reliability of functional transcranial Doppler ultrasonography. *Ultrasound Med Biol* 27: 509–514, 2001.
40. **Weiller C, Juptner M, Fellows S, Rijntjes M, Leonhardt G, Kiebel S, Muller S, Diener HC, Thilmann AF.** Brain representation of active and passive movements. *Neuroimage* 4: 105–110, 1996.

